

Gβγ directly modulates vesicle fusion by competing with synaptotagmin for binding to neuronal SNARE proteins embedded in membranes.

Zack Zurawski<sup>1</sup>, Brian Page<sup>2</sup>, Michael C. Chicka<sup>3</sup>, Rebecca L. Brindley<sup>4</sup>, Christopher A. Wells<sup>1</sup>, Anita M. Preininger<sup>1</sup>, Karren Hyde<sup>1</sup>, James A. Gilbert<sup>1</sup>, Osvaldo Cruz-Rodriguez<sup>5</sup>, Kevin P. M. Currie<sup>1,4</sup>, Edwin R. Chapman<sup>3</sup>, Simon Alford<sup>2</sup>, and Heidi E. Hamm<sup>1</sup>

\*Running title: Gβγ-mediated inhibition of exocytosis in lipid membranes

<sup>1</sup>Department of Pharmacology, Vanderbilt University, Nashville, TN 37232-6600;

<sup>2</sup>Department of Anatomy and Cell Biology, University of Illinois at Chicago, Chicago, IL 60612-7308;

<sup>3</sup>Howard Hughes Medical Institute and Department of Neuroscience, University of Wisconsin, Madison, Wisconsin, 53705;

<sup>4</sup>Department of Anesthesiology, Vanderbilt University Medical Center, Nashville, TN 37232-6600;

<sup>5</sup>Departments of Pharmacology and Biological Chemistry, Life Sciences Institute, University of Michigan, Ann Arbor, Michigan 48109

To whom correspondence should be addressed: Heidi E. Hamm, Department of Pharmacology, Vanderbilt University Medical Center, 442 Robinson Research Building, 23rd Ave. South @ Pierce, Nashville, TN, USA, Tel.: (615) 343-3533; Fax: (615)-343-1084; E-mail: heidi.hamm@vanderbilt.edu

**Keywords:** G protein, G protein coupled receptor, SNARE proteins, exocytosis, neurotransmitter release

## ABSTRACT

G<sub>i/o</sub>-coupled GPCRs can inhibit neurotransmitter release at synapses via multiple mechanisms. In addition to Gβγ-mediated modulation of voltage-gated calcium channels (VGCC), inhibition can also be mediated through the direct interaction of Gβγ subunits with the soluble N-ethylmaleimide attachment protein receptor (SNARE) complex of the vesicle fusion apparatus. Binding studies with soluble SNARE complexes have shown that Gβγ binds to both ternary SNARE complexes, t-SNARE heterodimers, and monomeric SNAREs, competing with synaptotagmin(syt)1 for binding sites on t-SNARE. However, in secretory cells, Gβγ, SNAREs, and synaptotagmin interact in the lipid environment of a vesicle at the plasma membrane. To approximate this environment, we show that fluorescently-labeled Gβγ interacts specifically with lipid-embedded t-SNAREs consisting of full-length syntaxin 1 and SNAP-25B at the membrane, as measured by fluorescence polarization. Fluorescently-labeled syt 1 undergoes competition with Gβγ for

SNARE binding sites in lipid environments. Mutant Gβγ subunits that were previously shown to be more efficacious at inhibiting Ca<sup>2+</sup>-triggered exocytotic release than wild-type Gβγ were also shown to bind SNAREs at higher affinity than wild-type in a lipid environment. These mutant Gβγ subunits were unable to inhibit VGCC currents. Specific peptides, corresponding to regions on Gβ and Gγ shown to be important for the interaction, disrupt the interaction in a concentration-dependent manner. In *in vitro* fusion assays utilizing full-length t- and v-SNAREs embedded in liposomes, Gβγ inhibited Ca<sup>2+</sup>/synaptotagmin-dependent fusion. Together, these studies demonstrate the importance of these regions for the Gβγ-SNARE interaction, and show that the target of Gβγ, downstream of VGCC, is the membrane-embedded SNARE complex.

## INTRODUCTION

Release of neurotransmitter into the synapse is an intricate synchronized process involving core exocytotic machinery proteins, ion channels, calcium sensors, presynaptic

inhibitory  $G_{i/o}$ -coupled receptors (GPCRs), and accessory proteins that each play a role in facilitating or inhibiting the docking, priming, and fusion of synaptic vesicles(1-3). The core exocytotic machinery consists of three members of a group of proteins known as soluble N-ethylmaleimide-sensitive factor attachment protein receptors (SNAREs) (2,4,5). On the vesicle, the SNARE protein (v-SNARE) is vesicle-associated membrane protein-2 (VAMP2), also known as synaptobrevin. Within its sequence is a SNARE motif that forms an  $\alpha$ -helix that binds to the coiled-coil SNARE motifs in the dimer of two target membrane SNARE proteins (t-SNAREs), syntaxin1A and SNAP-25. SNAP-25 has within its sequence two SNARE motifs, so the full ternary SNARE complex comprises syntaxin1A, SNAP-25, and VAMP2 through association of these four  $\alpha$ -helical SNARE motifs(5).

Many other proteins have been shown to interact with either the SNARE proteins individually, the t-SNARE dimer, or the full ternary SNARE. The components of minimal membrane fusion are thought to be the SNAREs, synaptotagmin, the SM proteins (nSec1, Munc18), Munc13, and complexin(2,3). Calcium sensor proteins respond to the increase in calcium concentration resulting from the activation of voltage-gated calcium channels and promote the fusion of the vesicle with the target membrane. One group of calcium sensors of particular interest are the synaptotagmins. In neurons, it is currently believed that a major calcium sensor for exocytosis is synaptotagmin 1, containing an N-terminal intraluminal domain, a transmembrane domain, and a tandem set of calcium-binding C2-domains termed C2A and C2B(6-8). While synaptotagmin can bind syntaxin1A and SNAP25 with low affinity in the absence of calcium, its affinity increases markedly in the presence of elevated calcium levels(9-11). Synaptotagmin 1 binds lipids in addition to SNAREs, with both phosphatidylserine and  $PIP_2$  being essential for the function of the full-length protein (9,12-14). The lipid-binding and SNARE-binding functionalities of synaptotagmin are both essential for its role in mediating fast synchronous release at the synapse.

Activation of inhibitory  $G_{i/o}$ -coupled G protein coupled receptors (GPCRs) causes inhibition of exocytosis through several mechanisms. GPCRs signal through heterotrimeric G proteins, with both the guanine nucleotide-binding  $G\alpha$  subunit and the  $G\beta\gamma$  subunit implicated in discrete signaling pathways(1,15). While the best-studied mechanism involves the inhibition of adenylyl cyclase by  $G\alpha_i$ , the  $G\beta\gamma$  heterodimer is also capable of inhibiting exocytosis in several ways. A large number of independent groups have shown that  $G\beta\gamma$  can inhibit calcium currents through direct binding to  $Ca_v2$  (N- P/Q- and R-type) voltage-gated calcium channels(16-19). This mechanism of inhibition is found at a large number of synapses, including certain subtypes of GPCRs thought to work entirely via it(20-22). Inhibition of exocytosis by  $G_{i/o}$ -coupled GPCRs downstream of calcium entry is also known to occur(23-26). It has been shown by multiple independent groups that  $G\beta\gamma$  binds to the SNARE complex to inhibit exocytosis downstream of calcium entry(27-31). Electrophysiological and *in vitro* protein binding studies have shown that the C-terminus of SNAP-25 is a critical binding site for this interaction(30-32). We propose that  $G\beta\gamma$  competes with synaptotagmin 1 for binding sites on SNAP-25, disrupting the ability of synaptotagmin 1 to promote vesicle fusion in response to elevated intracellular calcium(28-30). This hypothesis is in line with current crystallographic structures of the synaptotagmin-SNARE interaction, featuring significant overlap between the known synaptotagmin 1 binding site and key  $G\beta\gamma$ -binding residues on the second helix of SNAP-25 that would be expected to produce a steric clash(30,33,34). Each inhibitory GPCR may signal via one or more of these mechanisms to achieve precise spatial and temporal control over neurotransmitter release: for example, the  $GABA_B$  receptor in the CA1 axons of the hippocampus signals via modulation of calcium currents, while the  $5-HT_{1B}$  receptor signals only downstream of calcium entry(20). This mechanism downstream of calcium entry has been reported to occur at a variety of inhibitory  $G_{i/o}$ -coupled GPCRs in a variety of secretory cell types(35-41),

demonstrating its importance for the regulation of exocytosis.

Prior protein biochemical studies elucidating the interplay between Gβγ, synaptotagmin, and SNAREs have been conducted in aqueous environments in the presence of detergent, and it has never been determined whether Gβγ can bind to SNAREs and directly inhibit vesicle fusion in lipid bilayers(28-31). In addition, the molecular requirements for the binding of SNARE proteins to Gβγ are not well-understood. It has been demonstrated that Gβ<sub>1</sub>γ<sub>2</sub> has a higher affinity than Gβ<sub>1</sub>γ<sub>1</sub> for t-SNARE complexes and is more efficacious at inhibiting fusion in permeabilized PC12 cells(28), but the regions on Gγ2 responsible for the 20-fold tighter interaction are not known. While a number of residues on SNARE have been shown to be important for Gβγ binding(30,31), the individual residues on Gβγ implicated in the SNARE interaction have yet to be identified.

Here, we have explored further the complex interplay between Gβγ and synaptotagmin 1 for the regulation of SNARE-driven fusion. We expand on previous differences noted between Gβγ isoforms in this mechanism and highlight the importance of a single residue, W332, on Gβ, for the interaction of Gβγ not only with SNAREs, but also voltage-gated calcium channels. Furthermore, we examine the ability of Gβγ to compete with synaptotagmin for association with SNARE-containing liposomes as well as demonstrate a role for this inhibition as it relates to fusion *in vitro*.

## RESULTS

Previous studies of Gβγ-SNARE interactions used recombinant soluble SNARE complexes in aqueous solution to show that Gβγ binds to ternary SNARE complexes, t-SNARE heterodimers, and the monomeric SNARE proteins SNAP25, syntaxin1A, and VAMP2(28-30). To examine binding of Gβγ to full-length t-SNARE complexes embedded in lipid bilayers, we developed an assay utilizing total internal reflection (TIRF) fluorescence intensity, and anisotropy (**Fig. 1A**). Purified Gβγ subunits fluorescently labeled at primary amine residues with Alexa Fluor 488 N-hydroxysuccinimide

ester were applied from a pipette over a t-SNARE-containing (syntaxin1A and SNAP-25) bilayer on a cover slip illuminated with TIRF or epifluorescence. During pulses of Gβ<sub>1</sub>γ<sub>1</sub>, there was a small increase in TIRF fluorescence measured at a photomultiplier in the absence of t-SNARE complexes; if t-SNAREs were present, this increase was an order of magnitude larger (**Fig 1B**). To confirm that this interaction represented binding of Gβγ to a target in the lipid bilayer, anisotropy of the fluorescence TIRF signal was measured (**Fig 1B**). Laser TIRF excitation was polarized and emission polarization was detected parallel and orthogonal to this excitation polarization. Immediately after Gβγ pressure ejection (which lasted for 1 s; **Fig 1B** grey bar), no increase in anisotropy of the fluorescence signal was observed if no t-SNARE was present, whereas in the presence of t-SNAREs, there was a large increase in anisotropy (**Fig. 1B inset**). The difference between the two conditions was significant.

The amplitude of the TIRF fluorescence response to Gβγ pressure application over the bilayer was used to quantify t-SNARE interactions of various Gβγ subtypes. Gβγ concentration at the lipid bilayer was calculated using epifluorescence of Gβγ at known concentrations in the solution above the lipid bilayer and comparing that value to epifluorescence of pressure ejected Gβγ (**Fig 1Ci**). Dosing to saturation was obtained by increasing concentrations of Gβγ in the pressure ejection pipette. A concentration response curve was constructed comparing Gβ<sub>1</sub>γ<sub>1</sub> to Gβ<sub>1</sub>γ<sub>2</sub>. We observed a 14-fold difference in affinity between Gβ<sub>1</sub>γ<sub>1</sub> and Gβ<sub>1</sub>γ<sub>2</sub> isoforms. These results confirmed results obtained for binding in aqueous solution(28,29). Gβγ subunits containing Ala mutations of two residues on the Gα-binding surface of Gβ, K78 and W332, inhibited exocytosis at a significantly higher potency than wild-type(28). To determine if this was due to increased affinity for t-SNAREs, we tested this mutant Gβ<sub>1</sub>γ<sub>2</sub> subunit in the TIRF assay. Gβ<sub>1</sub> K78A/W332Aγ<sub>2</sub> (**Fig 1D**, red curve) exhibited a significantly higher 1.7-fold increase in affinity for t-SNARE complexes compared to wild-type Gβ<sub>1</sub>γ<sub>2</sub>. Consistent with saturation of

binding leaving excess unbound Gβγ, anisotropy of these fluorescence signals decreased as the pressure ejected Gβγ concentrations were increased and the intensity signal saturated (data not shown).

To determine whether synaptotagmin could compete with Gβ<sub>1</sub>γ<sub>1</sub> in lipid membranes, we labeled recombinant synaptotagmin 1 C2AB with Alexa Fluor 488-C5-maleimide selectively on the lone Cys residue present in the sequence (Cys277). Alexa Fluor 488-synaptotagmin 1 was applied to coverslips coated with t-SNARE complexes consisting of purified recombinant syntaxin1A and SNAP-25 embedded in lipid membranes illuminated by TIRF. The anisotropy of the fluorescence TIRF signal produced via the binding of fluorescent synaptotagmin 1 to t-SNARE was recorded (**Fig. 2A**). Application of Ca<sup>2+</sup> increased the anisotropy of the fluorescent TIRF signal in a saturable manner produced by application of fluorescent synaptotagmin 1 to the t-SNARE containing bilayer (**Fig. 2B**). The rise in anisotropy produced via the binding of synaptotagmin 1 to t-SNARE complexes could be reversed in a concentration-dependent manner by purified Gβ<sub>1</sub>γ<sub>1</sub> (**Fig. 2C**).

To investigate whether the ability of Gβ<sub>1</sub>K78A/W332Aγ<sub>2</sub> and its corresponding single-Ala mutants to inhibit voltage-gated calcium currents was correspondingly enhanced, we conducted electrophysiological studies in HEK cells expressing Ca<sub>v</sub>2.2 (N-type) calcium channels along with wild-type Gβ<sub>1</sub>γ<sub>2</sub>, Gβ<sub>1</sub>K78A/W332Aγ<sub>2</sub>, Gβ<sub>1</sub>K78Aγ<sub>2</sub>, or Gβ<sub>1</sub>W332Aγ<sub>2</sub> (**Fig. 3**). Gβγ-mediated inhibition of Ca<sub>v</sub>2.2 channels is voltage-dependent; the inhibition is less pronounced at more depolarized test potentials and is transiently reversed by a conditioning prepulse to very depolarized potentials(42). This reversal (also called pre-pulse facilitation) is thought to reflect transient dissociation of Gβγ from the channel at the depolarized membrane potential. The magnitude of pre-pulse facilitation can therefore be used to quantify the extent of Gβγ-mediated inhibition of I<sub>Ca</sub>. We used a double pulse protocol (**Fig. 3A**) in which cells voltage-clamped at -80mV were stimulated by two identical test pulses (P1 and P2) to various potentials (-10mV, 0mV, +10mV and

+20mV). The second test pulse (P2) was preceded by a conditioning prepulse to +120mV to maximally reverse any Gβγ-mediated inhibition. In control conditions lacking Gβγ overexpression, there was a slight prepulse facilitation due to the presence of endogenous Gβγ(43). Robust prepulse facilitation and inhibition of I<sub>Ca</sub> was observed with co-expression of Gβγ. The magnitude of prepulse facilitation was diminished at more depolarized test potentials (**Fig. 3B**), consistent with the known reduction of Gβγ-mediated inhibition at depolarized test potentials(42). Compared to cells expressing wild type Gβγ, prepulse facilitation was only modestly affected in cells expressing the K78A mutant, but was abolished in cells expressing the W332A mutant (**Fig. 3B**). The K78A/W332A double mutant produced slight prepulse facilitation of I<sub>Ca</sub> that was not statistically different from control cells (**Fig. 3B**). These studies, in tandem with those conducted in **Fig. 1**, suggest that the W332A mutation and the K78A/ W332A double mutant dramatically reduce the ability of Gβ<sub>1</sub>γ<sub>2</sub> to interact with Ca<sub>v</sub>2.2 channels, and that the increased potency of the Gβ<sub>1</sub>K78A/W332Aγ<sub>2</sub> double mutant in the cracked PC12 cell assay is due to the enhanced interaction of Gβ<sub>1</sub>K78A/W332Aγ<sub>2</sub> with SNAREs.

To identify important regions on Gβ and Gγ for the binding of SNAP25, we utilized a peptide-competition approach to examine whether peptides derived from the primary sequence of Gβ<sub>1</sub>, Gγ<sub>1</sub> or Gγ<sub>2</sub> could disrupt the interaction between full-length Gβγ and SNAP25. We measured the ability of peptides to disrupt the interaction between full-length Gβ<sub>1</sub>γ<sub>2</sub> with SNAP25 utilizing the Alphascreen competition binding assay(31). Gβ<sub>1</sub> peptide 328-337, which contains W332, is a reasonably potent inhibitor of Gβ<sub>1</sub>γ<sub>2</sub> SNAP25 interaction (**Fig. 4A**), however, peptides corresponding to Gβ<sub>1</sub> peptides 86-98 and 243-251 did not inhibit the interaction. Peptides from Gγ subunits could also compete with Gβ<sub>1</sub>γ<sub>2</sub>-SNAP-25 interactions: a peptide corresponding to the N-terminal 2-24 residues of Gγ<sub>2</sub> was much more potent than a corresponding peptide on Gγ<sub>1</sub> (**Fig. 4B-C**). Peptides corresponding to residues 8-25 on Gγ<sub>1</sub> inhibited the interaction with equivalent potency



to residues 9-28 on G $\gamma_2$ . In contrast, no inhibition was observed with peptides corresponding to residues 32-48 on G $\gamma_1$  or 29-45 on G $\gamma_2$ . These studies suggest that the region 328-337, including W332, on G $\beta_1$  is important for SNAP-25 binding, and the N-terminus of G $\gamma_2$  is responsible for G $\beta_1\gamma_2$ 's increased affinity for t-SNARE heterodimers. In **Fig. 5**, regions on G $\beta_1$ , G $\gamma_1$ , and G $\gamma_2$  shown to be involved in interactions with SNAP-25 are illustrated in red in the 3-dimensional X-ray crystallographic structures of the Gβγ subunit(44-46), while individual residues K78 and W332 are depicted in blue.

To determine whether Gβγ subunits can inhibit SNARE-catalyzed liposome fusion in the presence of synaptotagmin-1, we performed reconstituted fusion assays similar to those conducted in previous studies(47-50). Liposomes containing v-SNAREs were prepared using recombinant full-length VAMP2 and a FRET donor-acceptor pair consisting of NBD-phosphatidylethanolamine(PE) and rhodamine-PE. t-SNARE liposomes were prepared containing full-length recombinant rat syntaxin 1A and SNAP-25B heterodimers. As the quenched FRET-pair containing liposomes fuse with the unlabeled liposomes, the concentration of the FRET acceptor rhodamine in the liposome is lowered, resulting in an increase in NBD donor fluorescence, as measured with an excitation wavelength of 460nm and an emission wavelength of 538nm (**Fig. 6A**). The cytoplasmic domain of synaptotagmin 1 (C2AB, 10  $\mu$ M (50)) stimulated fusion in the presence of 1 mM Ca $^{2+}$  (**Fig. 6B, black lines**). The extent and maximum rate of fusion obtained in the presence of both Ca $^{2+}$  and synaptotagmin 1 was substantially greater than in the absence of either component (data not shown). Purified bovine G $\beta_1\gamma_1$ , as well as recombinant His-tagged G $\beta_1\gamma_2$  purified from SF9 cells, inhibited Ca $^{2+}$ -synaptotagmin-1 triggered fusion in a concentration-dependent manner with reductions in both the slope and maximal levels of fusion(**Fig. 6B, blue and green lines**). The potency for G $\beta_1\gamma_2$  inhibition of Ca $^{2+}$  and SNARE-dependent synaptotagmin 1-driven lipid mixing was 14.5-fold higher than for G $\beta_1\gamma_1$  (**Fig. 6C**). Maximal concentrations of G $\beta_1\gamma_1$  reduced

fusion to a baseline level, comparable to conditions lacking synaptotagmin 1 or Ca $^{2+}$ . In the absence of synaptotagmin 1, G $\beta_1\gamma_1$  did not additionally inhibit fusion (**Fig. 6D**) indicating that the effect of Gβγ is to inhibit synaptotagmin 1-stimulated fusion.

To investigate whether Gβγ had higher potency at alternative concentrations of synaptotagmin 1, we performed reconstituted fusion assays similar to those in **Fig. 6C** with a lower concentration of synaptotagmin 1 (3.16  $\mu$ M) at 1mM Ca $^{2+}$ . G $\beta_1\gamma_1$  was found to inhibit fusion 1.8-fold more potently in a concentration-dependent manner at this reduced concentration of synaptotagmin 1 (**Fig. 6E**).

## DISCUSSION

Multiple independent groups have reported that the Gβγ-SNARE interaction is one of several important mechanisms through which G $\beta_1\gamma_2$ -coupled GPCRs inhibit exocytosis(35-38), along with inhibition of Ca $^{2+}$  influx by Gβγ through voltage-gated calcium channels. Mutagenesis studies have provided some of the strongest arguments in favor of this hypothesis: mutant forms of SNAP-25 that are unable to efficiently bind Gβγ are also unable to support G $\beta_1\gamma_2$ -coupled GPCR-mediated inhibition of exocytosis(30), and partial loss-of-function SNAP-25 mutants, with decreased Gβγ binding, show concomitant partially reduced G $\beta_1\gamma_2$ -coupled GPCR-mediated inhibition in the same populations of neurons(31). The heterogeneous nature of cellular systems prevents ruling out the possibility that an alternative effector for exocytosis, that utilizes the same residues in SNAP-25, is similarly perturbed. Here, we provide strong evidence against this idea by showing that Gβγ inhibits synaptotagmin-1-regulated, SNARE-catalyzed liposome fusion in a purified system lacking any other proteinaceous components. A concentration-dependence for G $\beta_1\gamma_2$  inhibition was observed, with an IC $_{50}$  of 157 nM. Other components, such as voltage-gated calcium channels and adenylyl cyclases, are entirely absent. From these and prior studies, it can be concluded that G $\beta_1\gamma_1$  and G $\beta_1\gamma_2$  both bind SNAREs, including monomeric

syntrophin1A, SNAP25, t-SNARE heterodimers, and/or VAMP2, incorporated into lipid bilayers, as determined here by fluorescence polarization, or previously in aqueous solution(28,29), and inhibits membrane fusion. The inhibitory effect of Gβγ on liposome fusion is only observed in the presence of Ca<sup>2+</sup>-synaptotagmin 1. The binding sites of Gβγ on SNAP-25 and synaptotagmin 1 on ternary SNAREs is known, encompassing overlapping but not identical regions(10,30,33). It has previously been shown that Gβγ competes with synaptotagmin 1 for binding sites on t-SNARE heterodimers and SNAP-25 in solution(28,29). From these prior studies in tandem with the competition binding studies conducted in **Fig. 2**, and our data showing that Gβγ has minimal effects on fusion in the absence of synaptotagmin 1 (**Fig. 6D**), we conclude that the inhibition of liposome fusion occurs directly via Gβγ binding to membrane-embedded SNAREs in a competitive manner with synaptotagmin 1. This observation corroborates and extends our previously published work(28-32). Despite this, it is clear that inhibition of voltage-gated calcium currents is an important mechanism through which Gβγ inhibits exocytosis for some, but not all, G<sub>i/o</sub>-coupled GPCRs(20,42).

While a considerable amount is known regarding the SNAP-25 residues that mediate binding to Gβγ (29-32), comparatively little is known concerning which residues of Gβγ mediate binding to SNARE proteins. It has been hypothesized that the SNARE-binding residues are located on the Gα-binding surface of Gβ, as heterotrimeric Gαβγ is incapable of binding SNAREs(29). Here, we validate and expand upon those results by demonstrating the role of W332 of Gβ in interaction with the SNARE complex and modulation of voltage-dependent calcium channels. This is a key Gα-binding residue required for heterotrimer assembly and receptor interaction as well as adenylyl cyclase activation(51). Strikingly, however, Ala mutation of this residue increases the potency of Gβγ inhibition of fusion in permeabilized PC12 cells(28), while abrogating modulation of voltage-dependent calcium channels. Strong linkage between this observation and the Gβγ-SNARE interaction has been generated here,

with the K78A/W332A double mutant of Gβ<sub>1</sub>γ<sub>2</sub> binding lipid-embedded t-SNAREs with significantly higher affinity than wild-type Gβ<sub>1</sub>γ<sub>2</sub>. Peptide binding studies expanded upon these studies, with a peptide Gβ<sub>1</sub> 328-337 corresponding to this region on Gβ<sub>1</sub> binding t-SNARE. Importantly, this peptide also inhibits the interaction of Gβ<sub>1</sub>γ<sub>2</sub> with SNAP25 in a concentration-dependent manner, while peptides corresponding to other regions of Gβ<sub>1</sub> do not.

Two key regions of interaction were identified on Gγ. In both this article (**Fig. 1**) and previous work(28), Gβ<sub>1</sub>γ<sub>2</sub> was shown to bind to t-SNARE complexes consisting of Stx1A and SNAP25 20-fold more tightly than Gβ<sub>1</sub>γ<sub>1</sub>. In **Fig. 4**, peptide competition data suggests that there is a SNAP-25-binding site in residues 9-28 of Gγ<sub>1</sub> and 8-25 of Gγ<sub>2</sub>, but a larger 2-24 peptide is 4.66-fold more potent than the 8-25 peptide. This suggests that the N-terminal residues 2-7 of Gγ<sub>2</sub> may be partially responsible for the increased ability of Gβ<sub>1</sub>γ<sub>2</sub> to bind t-SNARE.

The reduced ability of W332A mutants to inhibit voltage-gated calcium channels further supports the role of the Gβγ-SNARE binding in inhibition of exocytosis. Our results echo prior studies showing the W332A mutant dramatically reduced the Gβγ-mediated inhibition of *I<sub>Ca</sub>* (43,51)(**Fig. 3**). The double mutant K78A/W332A produced only slight inhibition of *I<sub>Ca</sub>*, with facilitation ratios not significantly different from control (no exogenous Gβγ) at any of the voltages tested (**Fig. 3B**). The K78A mutant has also been reported to reduce the inhibition of *I<sub>Ca</sub>* (51), although we found only a modest effect (**Fig. 3B**). That said, the inhibition produced by K78A was more sensitive to membrane potential; it produced significant inhibition (prepulse facilitation) at hyperpolarized test potentials but not at the more depolarized test pulses (**Fig. 3B**). This might suggest a modest reduction in binding affinity with K78A but we did not investigate this further in the present study.

The bulky tryptophan residue W332 has previously been shown to be inhibitory to certain classes of Gβ effectors, with enhanced βARK interaction previously reported for W332A mutants(51). In the X-ray crystallographic structure of βARK in complex

with Gβ<sub>1</sub>γ<sub>2</sub>(46,52), W332 is in close proximity to the α-helical C-terminus of βARK. Potentially, steric clashes may occur between W332 and K663 or N666 of βARK, which may be relieved in the W332A mutant. The enhanced binding affinity of W332A-containing mutant Gβγ for SNARE in *in vitro* binding assays supports a hypothesis that the side chain of W332 and/or K78 inhibit the interaction through steric clash and/or electrostatic repulsion with one of the K or R residues on the SNARE complex, such as R135, R136, R142, R161, R198, or K201 of SNAP25(30). In line with this hypothesis, a peptide corresponding to residues 548-671 of βARK blocks Gβγ-SNARE mediated inhibition of exocytosis(27). Charge-reversal of Gβγ-binding residues from Lys/Arg to Glu at the C-terminus of SNAP25 is far more destructive than neutral mutation to Ala(30,31), implying that negatively charged residues on Gβ or Gγ in addition to K78/W332 may contribute to the interaction.

Both direct binding assays and cell-based studies highlight the contribution of Gγ to the interaction, as Gβ<sub>1</sub>γ<sub>2</sub> binds SNAREs and inhibits exocytosis with an order of magnitude higher affinity than Gβ<sub>1</sub>γ<sub>1</sub>(28), despite the presence of identical Gβ in each complex. Two explanations for this phenomenon were hypothesized: specific residues on Gγ<sub>2</sub> have higher affinity for SNARE than those on Gγ<sub>1</sub>, or the C-terminal geranylgeranyl modification of Gγ<sub>2</sub>(53,54) contributes to the interaction more so than the farnesyl modification of Gγ<sub>1</sub>. We have localized the SNARE-binding residues to the N-terminus of Gγ<sub>2</sub> (**Fig. 5**), thus our data are supportive of the former hypothesis. Despite these studies, we have limited insights as to the specific binding mode of SNARE upon Gβγ. It is clear that X-ray crystallographic studies of the complete Gβγ-SNARE complex would yield tremendous insights as to the specific interplay of individual residues for the interaction.

In summary, we show that Gβγ subunits bind SNARE complexes in a lipid environment and inhibit fusion in a system containing only Gβγ, SNAREs, synaptotagmin 1, calcium and lipids. We highlighted residues and regions of importance on Gβ and Gγ for SNARE binding. These studies provide further evidence for the

Gβγ-SNARE hypothesis and highlight its importance in lipid bilayer-containing environments that more closely approximate the environment of the presynaptic active zone.

## EXPERIMENTAL PROCEDURES

**Plasmids-** The open reading frames for the SNARE component proteins were subcloned into the glutathione-s-transferase (GST) fusion vector, pGEX6p1, (GE Healthcare, Chalfont St. Giles, Buckinghamshire, UK) for expression in bacteria. The dual-expression vector pRSF-Duet1 with subcloned N-terminal His-tagged full length rat SNAP-25 and full length rat syntaxin1A was previously described(55). Full length bovine Gβ1 and His-tagged Gγ2 were incorporated in Sf9 vectors, described previously(51). The plasmid of a GST-fusion with rat synaptotagmin1(56), and the plasmid for the high affinity Gβ<sub>1</sub>γ<sub>2</sub> (K78A/W332A) were previously described(30). Voltage-gated calcium channel plasmids were as follows: bovine N-type Ca<sub>v</sub>2.2 (Genbank # NM174632; rat brain β<sub>2a</sub> (Genbank # M80545) ; rat α<sub>2δ</sub> (Genbank # M86621).

**Chemicals.** Unless otherwise specified, chemicals were obtained from Sigma-Aldrich. Accudenz® A.G., Cell Separation Media was obtained from Accurate Chemical & Scientific Co.

**Preparation and purification of recombinant proteins in E.coli.** Recombinant bacterially expressed syntaxin1A and 6xHisSNAP-25 were expressed in pRSF-Duet vector was transformed into *Escherichia coli* strain BL21. 6xHisVAMP2 was expressed in the plasmid pTW2. After initial starter culture overnight in LB media with 50 µg/ml of kanamycin (or ampicillin for pTW2), 4 liters of LB with antibiotic were inoculated with the starter culture and placed on a shaker at 37°C until an OD<sub>600</sub> of 0.8 was obtained. Protein expression was induced with 0.4 mM isopropyl β-D-thiogalactoside for an additional 4 h at 37°C. Bacterial cultures were pelleted, and then re-suspended in 10-15mls of resuspension buffer [25mM HEPES-KOH, pH 8.0; 400 mM KCl; 10 mM imidazole; and 5 mM β-mercaptoethanol]. After adding protease inhibitors (aprotinin, leupeptin, pepstatin, and phenylmethylsulfonyl fluoride, cells were



sonicated with a sonic dismembrator at 4°C for 2 cycles of 45 seconds with 45 seconds rest in between cycles. After sonication, 3 ml of 25% Triton X-100 was added to each tube and then incubated at 4°C on a rotator for 3-4 hours. These samples were then centrifuged to remove the insoluble material (25 minutes in a Beckman SW-34 rotor at 26,000 rpm). The supernatant was then purified via bulk affinity chromatography by mixing at 4°C overnight with cobalt-resin (Talon) pre-washed and equilibrated in resuspension buffer with the addition of 1% Triton X-100. The next day the beads were pelleted and washed twice with 5 volumes of OG wash buffer (25 mM HEPES-KOH, pH 8.0; 400 mM KCl; 20 mM imidazole; 5 mM β-mercaptoethanol; and 1% n-octylglucoside). After the second pelleting, the beads were then mixed at 4°C on a rotator with 5 volumes of elution buffer (25 mM HEPES-KOH, pH 8.0; 400 mM KCl; 200 mM imidazole; 5mM β-mercaptoethanol; 1% n-octylglucoside; and 10% glycerol) for 2 hours. The samples were pelleted to remove beads from the eluted protein. The protein concentrations were approximately determined with the Pierce 660nM Protein Assay (#22660, Thermo Scientific) and then confirmed for purity and concentration by SDS/PAGE analysis and comparison to a bovine serum albumin standard curve from the same gel. For synaptotagmin 1 purification, recombinant synaptotagmin 1 C2AB was prepared as a GST-fusion according to previously published methods(47), substituting the imidazole for recombinant human rhinovirus 3C protease to liberate the synaptotagmin 1 from the GST-tag.

**Gβγ Purification.** Gβ<sub>1</sub>γ<sub>1</sub> was purified from bovine retina as described previously(57). Recombinant Gβ<sub>1</sub>γ<sub>2</sub> was expressed in Sf9 cells and purified according to the method of Kozasa(58) with the following exceptions: frozen Sf9 cell pellets were lysed via sonication, with a duty cycle of 10 seconds followed by a resting period of 20 seconds, for 3 minutes at 30% intensity at 0°C. Gβ<sub>1.6xHis</sub>-γ<sub>2</sub> dimers were affinity-purified twice from detergent solubilized crude cell membrane using Talon® cobalt resin (Clontech) followed by three rounds of dialysis for a minimum of two hours in the following buffer: 20 mM HEPES-Na, pH 8.0

100 mM NaCl, 10mM 2-mercaptoethanol, 0.8% n-octylglucoside, 10% glycerol.

**Gβγ and Synaptotagmin 1 C2AB Labeling:** Purified Gβγ subunits were buffer exchanged into 20 mM HEPES pH 7.5, 100 mM NaCl, 1 mM MgCl<sub>2</sub>, 10 mM 2-mercaptoethanol, and 0.8% n-octylglucoside. Recombinant purified synaptotagmin 1 was buffer exchanged into 25 mM HEPES pH 7.4, 150 mM NaCl, 1 mM TCEP, and 10% glycerol. Alexa Fluor 488 NHS Ester (A20000, Invitrogen) or Alexa Fluor 488-C5-maleimide (A10254, Invitrogen) were prepared as a 10mM solution in DMSO. Proteins were labeled at a 20:1 probe:protein ratio for 1 hour. for all labeling reactions. For Gβγ, the reaction was then quenched via the addition of 50mM Tris-HCl and filtered through a 0.2μm polyethersulfone (PES) filter before being purified on a TSKgel G2000SW gel filtration column (TOSOH Biosciences). Fractions were collected and concentrated on an Amicon Ultra 10,000 MWCO centrifugal filter unit (Millipore) before being placed in a storage buffer consisting of 50 mM HEPES pH 7.6, 100 mM NaCl, 5 mM 2-mercaptoethanol, and 10% glycerol. For synaptotagmin 1 C2AB, the reaction was quenched via the addition of 5mM 2-mercaptoethanol and dialyzed to remove excess probe into 25 mM HEPES pH 7.8, 150 mM NaCl, 1 mM DTT, and 10% glycerol. Labeling stoichiometry was approximately 0.7-1 for synaptotagmin 1 C2AB and Gβγ.

**Preparation of liposomes for fusion and TIRF assays.** Protein-free and t-SNARE embedded liposomes were made as described previously(47,48). Briefly, a mixture of 55% POPC (1-Palmitoyl-2-Oleoyl-sn-glycero-3-phosphocholine), 15% DOPS (1,2-dioleoyl-sn-glycero-3-phospho-L-serine (sodium salt) and 30% POPE (1-Palmitoyl-2-Oleoyl-sn-glycero-3-phosphoethanolamine) in chloroform that would be equal to 15 mM of lipids in 100 μl was dried down. All lipids were purchased from Avanti Polar Lipids (Alabaster, Alabama). To this, either elution buffer (25 mM HEPES-KOH; pH 7.8, 400 mM KCl, 500 mM imidazole, 10% glycerol, 5 mM 2-mercaptoethanol, 1% n-octylglucoside) alone or with 0.4 mg of t-SNARE dimer was added to each tube of lipids to a final volume of 500 μl. For v-SNARE-



containing liposomes, 1.5% 1.5% N-(7-nitro-2-1,3-benzoxadiazol-4-yl)-1,2-dipalmitoyl phosphatidylethanolamine (NBD-PE) and 1.5% N-(lissamine rhodamine B sulfonyl)-1,2-dipalmitoyl phosphatidylethanolamine (Rhodamine-PE) were added to a mixture of 55% POPC/15% DOPS/27% POPC before drying down and .095 mg of recombinant 6xHis-tagged VAMP2 was added in elution buffer. These mixtures were agitated on a tabletop vortex until the lipids were dissolved (10-15 min). After lipids were dissolved, 2 volumes of reconstitution buffer (25 mM HEPES-KOH, pH 7.8; 100 mM KCl; 10% glycerol; 1mM DTT) was added dropwise and the sample was vortexed gently for another 10 minutes. After 10 minutes, the sample was transferred to dialysis tubing (10,000 molecular weight cutoff, ThermoScientific) and dialyzed overnight with two dialysis buffer exchanges after 6 hours. The dialysis buffer contained 25 mM HEPES-KOH, pH 7.8; 100 mM KCl; 10% glycerol; and 1 mM DTT. Gradients were assembled in thin-walled centrifuge tubes (#344057, Beckman Coulter) for a SW-55 swinging bucket rotor (Beckman Coulter), with 1.5ml of the lipid/Accudenz mixture at the bottom, 1.5 ml of 30% Accudenz, and finally 450μl of 0% Accudenz on the top. Liposomes were floated via centrifugation at 55,000 rpm for 2 hours at 4°C with minimal brake. Liposomes can be visualized as a thin uniform layer of opacity at the 0-30% interface of the gradient. Approximately 0.4ml of liposomes were removed from each layer by direct puncture with a 27 gauge needle at the 0%-30% Accudenz interface. All tubes from each preparation were mixed, aliquoted, and flash-frozen with an ethanol/dry ice bath. Liposomes were stored at -80°C. Lipid concentrations and recovery rates were quantified using the Beer-Lambert law from NBD-PE absorbance values at 460nm from liposomes containing NBD-PE that were diluted with docdeylmaltoside to 0.5%. SNARE protein concentrations in liposomes were determined via Coomassie Brilliant Blue R-250 staining of

SDS-PAGE gels containing a standard curve of known concentrations of bovine serum albumin (Thermo Scientific) followed by densitometric analysis utilizing the Fiji distribution of ImageJ software(59,60). SNARE copy number was determined according to previously published methods(47).

*In membrane TIRF imaging:* Bilayers were prepared from 55% PC, 15% PS, 29% PE, and 1% DiO liposomes with or without t-SNARE complexes as above except DiO (1%) was added. Cover slips were cleaned by soaking in 2% Hellmanex II solution, sonicated at (50°C), rinsed in 18 MΩ deionized water and in 100% ethanol and stored in ethanol. For recording, cover slips were rinsed, dried under filtered compressed air, and placed in a microscope recording chamber. 650 μl of HEPES-KCl was added to 100 μl of proteoliposome mix, and then 750 μl of HEPES-KCl with 10 mM CaCl<sub>2</sub>. 25 μL of this mixture was placed in the cover slip chamber and let sit for 1 hour to allow a lipid bilayer to settle on the cover slip. This lipid bilayer was washed with a superfusate of 290mM HEPES-KCl and 10mM EGTA titrated with CaCl<sub>2</sub> to a final free Ca<sup>2+</sup> concentration of 100nM). The DiO fluorescent bilayer was excited using laser TIRF microscopy under a 60X 1.45 NA lens (Olympus Plan-APO-N). This enabled the correct focal plane to be attained and alignment of the TIRF laser angle. DiO fluorescence was then bleached to extinction by continuous excitation (20 mins). Gβγ labeled with Alexa 488 (see above) was pressure ejected from a pipet over the bilayer to obtain a transient exposure of Gβγ to the lipid bilayer and the intensity of fluorescence excited with TIRF illumination was then measured with photomultipliers while Gβγ concentrations and subtype were varied in the pipette. The concentration of Gβγ over the bilayer was measured by conventional epifluorescence through the cover slip and the resulting signal amplitude was compared to known concentrations of labeled Gβγ in the recording chamber. In some experiments fluorescence anisotropy was also recorded to confirm protein-protein interactions occurred. This was achieved by measuring fluorescence through a polarizing beamsplitter with detector parallel and

orthogonal to the plane of the TIRF laser plane polarization angle.

**HEK cell culture and transfection:** HEK293 cells were maintained in an incubator at 37°C and 5% CO<sub>2</sub> and were passaged every 3-4 days for up to 15 passages. Cells were cultured in Minimum Essential Media (MEM; Life Technologies, Grand Island, NY) supplemented with fetal bovine serum (10%; GE Healthcare Life Sciences, Logan, UT), L-glutamine (2mM; Life Technologies, Grand Island, NY) and penicillin / streptomycin (100 unit ml<sup>-1</sup> / 100μg ml<sup>-1</sup>; Mediatech Inc., Manassas, VA). 24 hours before transfection, cells were plated in 35mm dishes according to manufacturer's guidelines for Lipofectamine 2000 (Invitrogen, Grand Island, NY) transfection. Cells were transiently transfected with voltage-gated calcium channel subunits Ca<sub>v</sub>2.2, β<sub>2a</sub>, α<sub>2δ</sub> alongside Gβ<sub>1</sub> (either WT, K78A, W332A or K78A/W332A) and Gγ<sub>2</sub> subunits in a 1:1:1:3:3 ratio respectively. Some control cells were transfected with only the voltage-gated calcium channel subunits. Transfected cells were visually identified by GFP expressed downstream of an IRES sequence in the β<sub>2a</sub> subunit plasmid. Cells were re-plated onto poly-L-lysine coated coverslips 48-60 hours after transfection and left to adhere for 2 hours before patch clamp electrophysiology experiments.

**Patch clamp electrophysiology experiments-** Transfected HEK cells were recorded in the whole cell patch clamp configuration and all experiments were performed at room temperature. Patch pipette electrodes were pulled from borosilicate glass capillary tubes (World Precision Instruments, Sarasota, FL) using a Sutter P-97 pipette puller (Sutter Instruments, Novato, CA), coated with dental wax (Electron Microscopy Services, Hatfield, PA) and fire polished using a Narishige MF-830 micro forge (Narishige, Amityville, NY). Pipette resistance was ~ 2MΩ when filled with internal patch pipette solution containing (in mM) 110 CsCl, 4 MgCl<sub>2</sub>.6H<sub>2</sub>O, 20 HEPES, 10 EGTA, 4 MgATP, 0.35 Na<sub>2</sub>GTP, 14 creatine phosphate, pH7.3, osmolarity ~305-310 mOsm. Coverslips were placed in a recording bath, continually perfused with extracellular solution at a rate of ~ 3mls/min and cells viewed on a Nikon TE2000 inverted microscope. Cells were

initially washed in a NaCl based extracellular solution consisting of (in mM) 145 NaCl, 2 KCl, 1 MgCl<sub>2</sub>.6H<sub>2</sub>O, 10 glucose, 10 HEPES, 2 CaCl<sub>2</sub>, pH 7.3, osmolarity ~ 305 mOsm. After obtaining the whole cell recording configuration the extracellular solution was a tetraethyl ammonium chloride based (TEACl) one containing (in mM) 145 TEACl, 10 HEPES, 10 glucose, 1 MgCl<sub>2</sub>.6H<sub>2</sub>O, 5 BaCl<sub>2</sub>, pH 7.3, osmolarity ~ 305 mOsm. Transfected HEK cells were voltage clamped using an Axopatch 200B amplifier, Digidata 1400A interface and PClamp10 (Clampex) acquisition software (Molecular Devices, Sunnyvale, CA). A double pulse protocol was used to evoke voltage-gated calcium channel currents (*I<sub>Ca</sub>*). Cells were stimulated by two identical 20ms step depolarizations (P1 and P2) to various potentials (-10mV, 0mV, 10mV and + 20mV) from a holding potential of -80mV. The second test pulse (P2; 270ms after P1) was preceded by a 30ms conditioning prepulse to +120mV. Analog data were filtered at 2kHz and sampled at 20kHz. Series resistance was partially compensated (~60-70%) using the Axopatch circuitry and *I<sub>Ca</sub>* were subject to linear capacitance and leak subtraction using P/-8 protocols with leak pulses applied after test pulses. Raw data were analyzed in PClamp (Clampfit) software with *I<sub>Ca</sub>* amplitude measured 5ms after P1 or P2 test pulse onset. Graphing and statistical analysis were performed using OriginPro 7 (Originlab Corporation, Northampton, MA) and Prism 5 (GraphPad Software, Inc., La Jolla, CA) software. Statistical significance was determined using ANOVA with Dunnett's multiple pairwise comparison.

**Peptide synthesis-** Peptide array synthesis was performed using the ResPep SL peptide synthesizer (Intavis AG, Koeln, Germany) according to previously published automated SPOT synthesis methods(30,61). Peptides correspond to the primary amino acid sequence of the protein of interest on the GenBank database for human GNB1, GNNT1, or GNG2.

**Alphascreen Competition Binding Assays.** Alphascreen luminescence measurements were performed in an EnSpire multimode plate reader (Perkin-Elmer, Waltham MA) at 27°C. Biotinylated SNAP-25 was diluted to a 5x

concentration of 100nM in assay buffer (20 mM HEPES, pH 7.0, 10 mM NaCl, 40 mM KCl, 5% glycerol, and 0.01% triton X-100). An EC<sub>80</sub> concentration of 180nM of purified 6xHis-Gβ<sub>1</sub>γ<sub>2</sub> was made in assay buffer. Peptide stocks in DMSO were spotted onto 384-well white OptiPlates (Perkin-Elmer, Waltham, MA) at concentration ranges of 1nM to 100μM using a Labcyte Echo 555 Omics acoustic liquid handler (Labcyte, Sunnyvale, CA), with DMSO being back-added to a final concentration of 0.1%. 4μL of Gβ<sub>1</sub>γ<sub>2</sub> solution was incubated with peptide for 5m while shaking. After 5m, 1μL of biotinylated SNAP25 was added to a final concentration of 20nM. Subsequent to incubation while shaking for an additional 5m, 10μL of Alphascreen Histidine Detection Kit (Nickel Chelate) acceptor beads were added to a final concentration of 20ug/mL in assay buffer. The assay plate was agitated in dim light for 30m. At that point, Alphascreen Streptavidin Donor Beads were added to a final concentration of 20ug/mL in dim light. All aqueous solutions in this assay were manipulated via a Velocity 11 Bravo liquid handler (Agilent Automation Solutions, Santa Clara, CA). The final volume in the assay plate was 25μL. After being spun down briefly to settle all fluid at the bottom of the well, plates were incubated for an additional 1 hour at 27°C before being read in the EnSpire. 20nM biotinylated recombinant glutathione-S-transferase (*Schistosoma japonicum*) in place of SNAP-25 with Gβ<sub>1</sub>γ<sub>2</sub> were used as a negative control for non-specific binding in each assay. IC<sub>50</sub> concentrations for each peptide were determined by sigmoidal dose-response curve fitting with variable slope. To have a strong signal in the Alphascreen competition binding assay that could still be competed with a peptide, we used an EC<sub>80</sub> concentration (180nM) of 6xHis-tagged Gβ<sub>1</sub>γ<sub>2</sub> combined with 20nM recombinant human SNAP25 biotinylated on primary amine residues with NHS-biotin and increasing concentrations of peptides corresponding to a region on Gβ<sub>1</sub> or Gγ<sub>1</sub> in the Alphascreen bead assay. As a negative control, peptides were tested for their ability to disrupt a second Alphascreen assay in which donor and acceptor beads were reacted with 50nM of a

peptide consisting of a biotinylation site and a His-tag peptide (PerkinElmer, Waltham, MA).

**Reconstituted fusion/ lipid mixing assay.** 45 μL of t-SNARE liposomes were reacted with 5 μL of v-SNARE liposomes in a total of 75 μL of assay buffer (25mM HEPES-KOH, pH 7.8; 100mM KCl; 10% glycerol; 1mM DTT; 0.2mM ethyleneglycoltetraacetic acid (EGTA)) in white 96-well FluoroNunc plates (Thermo Fisher, Waltham, MA). Purified synaptotagmin 1 (10 μM) was added to the buffer along with a concentration-response curve of purified bovine Gβ<sub>1</sub>γ<sub>1</sub>, followed by the addition of the t-SNARE liposomes. All components of the fusion reaction, except v-SNARE vesicles, were combined, and pre-warmed to 37 C for 15 min. NBD fluorescence (excitation 460nm/emission 538nm) was continuously monitored over 80 m in a BioTek Synergy plate reader under continuous agitation, with fluorescence intensity being read every eight seconds. After 20 m, CaCl<sub>2</sub> was added to a final concentration of 1.2 mM in the assay, with 0.2 mM being chelated by EGTA to yield an effective concentration of 1.0 mM. After 80 m, dodecylmaltoside was added to a final concentration of 0.5% to maximally dequench NBD via infinite distance of the NBD:rhodamine FRET pair.

**Protein structure visualization:** All representatives of protein structure were made using Pymol.

**Statistics-** Two-tailed Student's t-tests and all concentration response-curve fitting sigmoidal dose-response with variable slope) were performed using GraphPad Prism v.4.03 for Windows, (GraphPad Software, La Jolla, California, USA, [www.graphpad.com](http://www.graphpad.com)). Sigmoidal dose-response curves were plotted using 1500 line segments. For the purposes of IC<sub>50</sub> estimation in sigmoidal concentration-response curves, all IC<sub>50</sub> values were calculated using an additional maximal point representing one order of magnitude above the highest concentration tested at the lowest signal value obtained in the study. For two-tailed Student's t-tests, *p* values < 0.05 were considered to be statistically significant. \* *p* < 0.05, \*\* *p* < 0.01.

**ACKNOWLEDGEMENTS:** We would like to thank Chantell S. Evans, Ph.D and Huan Bao, Ph.D for their expertise in conducting lipid mixing assays, as well as Jin Liao and James Gilbert for assistance in protein purification. We would like to thank the following labs for providing plasmids: Dr. Aaron Fox (University of Chicago, Chicago, IL); Dr. Roger Colbran (Vanderbilt University, Nashville, TN); Dr. Terry Snutch (University of British Columbia, Vancouver, Canada). Funding was provided by the R01 grant NIH (NINDS) R01NS052446, NIH (NEI) R01EY010291, NIH (NIMH) R01MH101679, NIH (NIMH) R01MH061876 and RO1MH084874. The content is solely the responsibility of the authors and does not necessarily represent the official views of the National Institutes of Health. E.R.C. is an Investigator of the Howard Hughes Medical Institute.

**CONFLICT OF INTEREST:** All authors declare that no conflicts of interest exist for them within the contents of this article.

**AUTHORSHIP CONTRIBUTIONS:** ZZ, BP, MCC, RLB, CAW, KPMC, ERC, SA, and HEH participated in research design. ZZ, BP, MCC, RLB, CAW, and SA conducted experiments. ZZ, CAW, AMP, KH, JAG, and OC-R contributed new reagents. ZZ, BP, MCC, RLB, CAW, KPMC, SA, and HEH performed data analysis. ZZ, KPMC, ERC, SA, and HEH wrote or contributed to the writing of the manuscript.

**ABBREVIATIONS USED:** GPCR: G protein coupled receptor. Gβγ: G protein betagamma subunit. SNARE: Soluble N-ethylmaleimide attachment protein receptor. SNAP-25: synaptosomal-associated protein of 25 kDa. SM: Sec1/Munc18. VAMP2: synaptobrevin Syt1 C2AB: the tandem C2A-C2B domain of synaptotagmin 1. HEK: Human embryonic kidney cells 293. TIRF: total internal reflection microscopy.

## REFERENCES

1. Betke, K. M. , Wells, C. A., Hamm, H. E. (2012) GPCR mediated regulation of synaptic transmission. *Prog Neurobiol.* **3**
2. Rizo, J., and Xu, J. (2015) The Synaptic Vesicle Release Machinery. *Annual Review of Biophysics* **44**, 339-367
3. Südhof, T. C. (2013) Neurotransmitter Release: The Last Millisecond in the Life of a Synaptic Vesicle. *Neuron* **80**, 675-690
4. Augustin, I., Rosenmund, C., Südhof, T. C., and Brose, N. (1999) Munc13-1 is essential for fusion competence of glutamatergic synaptic vesicles. *Nature* **400**, 457-461
5. Jahn, R., and Scheller, R. H. (2006) SNAREs [mdash] engines for membrane fusion. *Nat Rev Mol Cell Biol* **7**, 631-643
6. Chapman, E. R., and Jahn, R. (1994) Calcium-dependent interaction of the cytoplasmic region of synaptotagmin with membranes. Autonomous function of a single C2-homologous domain. *Journal of Biological Chemistry* **269**, 5735-5741
7. Perin, M. S., Fried, V. A., Mignery, G. A., Jahn, R., and Südhof, T. C. (1990) Phospholipid binding by a synaptic vesicle protein homologous to the regulatory region of protein kinase C. *Nature* **345**, 260-263
8. Rizo, J., and Südhof, T. C. (2012) The Membrane Fusion Enigma: SNAREs, Sec1/Munc18 Proteins, and Their Accomplices—Guilty as Charged? *Annual Review of Cell and Developmental Biology* **28**, 279-308
9. Chapman, E. R., Hanson, P. I., An, S., and Jahn, R. (1995) Ca<sup>2+</sup> regulates the interaction between synaptotagmin and syntaxin 1. *J Biol Chem* **270**, 23667-23671
10. Zhang, X., Kim-Miller, M. J., Fukuda, M., Kowalchyk, J. A., and Martin, T. F. (2002) Ca<sup>2+</sup>-dependent synaptotagmin binding to SNAP-25 is essential for Ca<sup>2+</sup>-triggered exocytosis. *Neuron* **34**, 599-611



11. Gerona, R. R., Larsen, E. C., Kowalchuk, J. A., and Martin, T. F. (2000) The C terminus of SNAP25 is essential for  $\text{Ca}^{2+}$ -dependent binding of synaptotagmin to SNARE complexes. *Journal of Biological Chemistry* **275**, 6328-6336
12. Wang, Z., Liu, H., Gu, Y., and Chapman, E. R. (2011) Reconstituted synaptotagmin I mediates vesicle docking, priming, and fusion. *The Journal of Cell Biology* **195**, 1159-1170
13. Liu, H., Bai, H., Xue, R., Takahashi, H., Edwardson, J. M., and Chapman, E. R. (2014) Linker mutations reveal the complexity of synaptotagmin 1 action during synaptic transmission. *Nat Neurosci* **17**, 670-677
14. Bai, J., Tucker, W. C., and Chapman, E. R. (2004) PIP2 increases the speed of response of synaptotagmin and steers its membrane-penetration activity toward the plasma membrane. *Nat Struct Mol Biol* **11**, 36-44
15. Oldham, W. M., and Hamm, H. E. (2008) Heterotrimeric G protein activation by G-protein-coupled receptors. *Nat Rev Mol Cell Biol* **9**, 60
16. Dunlap, K., Fischbach, G. D. (1978) Neurotransmitters decrease the calcium component of sensory neurone action potentials. *Nature* **276**, 837-839
17. Bean, B. P. (1989) Neurotransmitter inhibition of neuronal calcium currents by changes in channel voltage dependence. *Nature* **340**, 153-156
18. Herlitze, S., Garcia, D. E., Mackie, K., Hille, B., Scheuer, T., and Catterall, W. A. (1996) Modulation of  $\text{Ca}^{2+}$  channels by G-protein  $\beta\gamma$  subunits. *Nature* **380**, 258-262
19. Miller, R. J. (1998) Presynaptic receptors. *Annual Reviews in Pharmacology and Toxicology* **38**, 201-227
20. Hamid, E., Church, E., Wells, C. A., Zurawski, Z., Hamm, H. E., and Alford, S. Modulation of Neurotransmission by GPCRs Is Dependent upon the Microarchitecture of the Primed Vesicle Complex. *The Journal of Neuroscience* **34**, 260-274
21. Isaacson, J. S. (1998) GABA<sub>B</sub> Receptor-Mediated Modulation of Presynaptic Currents and Excitatory Transmission at a Fast Central Synapse. *Journal of Neurophysiology* **80**, 1571-1576
22. Takahashi, T., Kajikawa, Y., and Tsujimoto, T. (1998) G-Protein-Coupled Modulation of Presynaptic Calcium Currents and Transmitter Release by a GABA<sub>B</sub> Receptor. *The Journal of Neuroscience* **18**, 3138-3146
23. Scanziani, M., Capogna, M., Gähwiler, B. H., and Thompson, S. M. (1992) Presynaptic inhibition of miniature excitatory synaptic currents by baclofen and adenosine in the hippocampus. *Neuron* **9**, 919-927
24. Wollheim, C. B., Kikuchi, M., Renold, A. E., and Sharp, G. W. G. (1977) Somatostatin- and Epinephrine-Induced Modifications of  $^{45}\text{Ca}^{++}$  Fluxes and Insulin Release in Rat Pancreatic Islets Maintained in Tissue Culture. *Journal of Clinical Investigation* **60**, 1165-1173
25. Mandarino, L., Itoh, M., Blanchard, W., Patton, G., and Gerich, J. (1980) Stimulation of Insulin Release in the Absence of Extracellular Calcium by Isobutylmethylxanthine and Its Inhibition by Somatostatin. *Endocrinology* **106**, 430-433
26. Silinsky, E. M. (1984) On the mechanism by which adenosine receptor activation inhibits the release of acetylcholine from motor nerve endings. *Journal of Physiology* **346**, 243-256
27. Blackmer, T., Larsen, E. C., Takahashi, M., Martin, T. F., Alford, S., and Hamm, H. E. (2001) G protein  $\beta\gamma$  subunit-mediated presynaptic inhibition: regulation of exocytotic fusion downstream of  $\text{Ca}^{2+}$  entry. *Science* **292**, 293-297.
28. Blackmer, T., Larsen, E. C., Bartleson, C., Kowalchuk, J. A., Yoon, E. J., Preininger, A. M., Alford, S., Hamm, H. E., and Martin, T. F. (2005) G protein  $\beta\gamma$  directly regulates SNARE protein fusion machinery for secretory granule exocytosis. *Nat Neurosci* **8**, 421-425
29. Yoon, E. J., Gerachshenko, T., Spiegelberg, B. D., Alford, S., and Hamm, H. E. (2007) Gβγ interferes with  $\text{Ca}^{2+}$ -dependent binding of synaptotagmin to the soluble N-ethylmaleimide-sensitive factor attachment protein receptor (SNARE) complex. *Mol. Pharmacol.* **72**, 1210-1219

30. Wells, C. A. , Zurawski, Z., Betke, K. M. , Yim, Y.Y., Hyde, K., Rodriguez, S., Alford, S., Hamm, H. E. (2012) Gβγ Inhibits Exocytosis Via Interaction with Critical Residues on SNAP-25. *Mol Pharmacol.* **82**, 1136-1149
31. Zurawski, Z., Rodriguez, S., Hyde, K., Alford, S., and Hamm, H. E. (2016) Gβγ Binds to the Extreme C Terminus of SNAP25 to Mediate the Action of Gi/o-Coupled G Protein–Coupled Receptors. *Molecular Pharmacology* **89**, 75-83
32. Gerachshenko, T., Blackmer, T., Yoon, E. J., Bartleson, C., Hamm, H. E., and Alford, S. (2005) Gbetagamma acts at the C terminus of SNAP-25 to mediate presynaptic inhibition. *Nat Neurosci* **8**, 597-605
33. Zhou, Q., Lai, Y., Bacaj, T., Zhao, M., Lyubimov, A. Y., Uervirojnangkoorn, M., Zeldin, O. B., Brewster, A. S., Sauter, N. K., Cohen, A. E., Soltis, S. M., Alonso-Mori, R., Chollet, M., Lemke, H. T., Pfuetzner, R. A., Choi, U. B., Weis, W. I., Diao, J., Sudhof, T. C., and Brunger, A. T. (2015) Architecture of the synaptotagmin-SNARE machinery for neuronal exocytosis. *Nature* **525**, 62-67
34. Brewer, K. D., Bacaj, T., Cavalli, A., Camilloni, C., Swarbrick, J. D., Liu, J., Zhou, A., Zhou, P., Barlow, N., Xu, J., Seven, A. B., Prinslow, E. A., Voleti, R., Haussinger, D., Bonvin, A. M. J. J., Tomchick, D. R., Vendruscolo, M., Graham, B., Sudhof, T. C., and Rizo, J. (2015) Dynamic binding mode of a Synaptotagmin-1-SNARE complex in solution. *Nat Struct Mol Biol* **22**, 555-564
35. Delaney AJ, C. J., Sah P. (2007) Noradrenaline modulates transmission at a central synapse by a presynaptic mechanism. *Neuron.* **5**, 880-892
36. Zhao, Y., Fang, Q., Straub, S. G., Lindau, M., and Sharp, G. W. G. (2010) Noradrenaline inhibits exocytosis via the G protein βγ subunit and refilling of the readily releasable granule pool via the α<sub>i</sub>1/2 subunit. *The Journal of Physiology* **588**, 3485-3498
37. Zhang, X.-l., Upreti, C., and Stanton, P. K. Gβγ and the C Terminus of SNAP-25 Are Necessary for Long-Term Depression of Transmitter Release. *PLoS ONE* **6**, e20500
38. Glitsch, M. (2006) Selective Inhibition of Spontaneous But Not Ca<sup>2+</sup>-Dependent Release Machinery by Presynaptic Group II mGluRs in Rat Cerebellar Slices. *Journal of Neurophysiology* **96**, 86
39. Iremonger, K. J., and Bains, J. S. (2009) Retrograde Opioid Signaling Regulates Glutamatergic Transmission in the Hypothalamus. *The Journal of Neuroscience* **29**, 7349
40. Yoon, E. J., Hamm, H.E., and Currie, K.P.M. (2008) G protein βγ subunits modulate the number and nature of exocytotic fusion events in adrenal chromaffin cells independent of calcium entry. *J Neurophysiol* **100**, 2929-2939.
41. Van Hook, M. J., Babai, N., Zurawski, Z., Young Yim, Y., Hamm, H. E., and Thoreson, W. B. (2017) A presynaptic group III mGluR recruits Gβγ/SNARE interactions to inhibit synaptic transmission by cone photoreceptors in the vertebrate retina. *The Journal of Neuroscience*
42. Zamponi, G. W., and Currie, K. P. M. (2013) Regulation of Ca(V)<sub>2</sub> calcium channels by G protein coupled receptors. *Biochimica et biophysica acta* **1828**, 1629-1643
43. McDavid, S., Currie, K. P. M. (2006) G-proteins modulate cumulative inactivation of N-type (Cav2.2) calcium channels. *The Journal of Neuroscience* **26**, 13373-13383
44. Sondek, J., Bohm, A., Lambright, D. G., Hamm, H. E., and Sigler, P. B. (1996) Crystal structure of a G-protein βγ dimer at 2.1Å resolution [see comments] [corrected] [published erratum appears in Nature 1996 Feb 29;379(6568):847]. *Nature* **379**, 369-374
45. Lambright, D. G., Sondek, J., Bohm, A., Skiba, N. P., Hamm, H. E., and Sigler, P. B. (1996) The 2.0 Å crystal structure of a heterotrimeric G protein [see comments]. *Nature* **379**, 311-319
46. Lodowski, D. T., Pitcher, J. A., Capel, W. D., Lefkowitz, R. J., and Tesmer, J. J. G. (2003) Keeping G proteins at bay: A complex between G protein-coupled receptor kinase 2 and Gβγ. *Science* **300**, 1256-1262

47. Tucker, W. C., Weber, T., and Chapman, E. R. (2004) Reconstitution of  $\text{Ca}^{2+}$ -regulated membrane fusion by synaptotagmin and SNAREs. *Science* **304**, 435-438
48. Weber, T., Zemelman, B. V., McNew, J. A., Westermann, B., Gmachl, M., Parlati, F., Sollner, T. H., and Rothman, J. E. (1998) SNAREpins: minimal machinery for membrane fusion. *Cell* **92**, 759-772
49. Bhalla, A., Chicka, M. C., Tucker, W. C., and Chapman, E. R. (2006)  $\text{Ca}^{2+}$ -synaptotagmin directly regulates t-SNARE function during reconstituted membrane fusion. *Nat Struct Mol Biol* **13**, 323-330
50. Gaffaney, J. D., Dunning, F. M., Wang, Z., Hui, E., and Chapman, E. R. (2008) Synaptotagmin C2B Domain Regulates  $\text{Ca}^{2+}$ -triggered Fusion in Vitro: CRITICAL RESIDUES REVEALED BY SCANNING ALANINE MUTAGENESIS. *Journal of Biological Chemistry* **283**, 31763-31775
51. Ford, C. E., Skiba, N. P., Bae, H., Daaka, Y., Reuveny, E., Shekter, L. R., Rosal, R., Weng, G., Yang, C. S., Iyengar, R., Miller, R. J., Jan, L. Y., Lefkowitz, R. J., and Hamm, H. E. (1998) Molecular basis for interactions of G protein  $\beta\gamma$  subunits with effectors. *Science* **280**, 1271-1274
52. Waldschmidt, H. V., Homan, K. T., Cruz-Rodríguez, O., Cato, M. C., Waninger-Saroni, J., Larimore, K. M., Cannavo, A., Song, J., Cheung, J. Y., Kirchhoff, P. D., Koch, W. J., Tesmer, J. J. G., and Larsen, S. D. (2016) Structure-Based Design, Synthesis, and Biological Evaluation of Highly Selective and Potent G Protein-Coupled Receptor Kinase 2 Inhibitors. *Journal of Medicinal Chemistry* **59**, 3793-3807
53. Simonds, W. F., Butrynski, J. E., Gautam, N., Unson, C. G., and Spiegel, A. M. (1991) G-protein  $\beta\gamma$  dimers. Membrane targeting requires subunit coexpression and intact gamma C-A-A-X domain. *Journal of Biological Chemistry* **266**, 5363-5366
54. Takida, S., and Wedegaertner, P. B. (2003) Heterotrimer Formation, Together with Isoprenylation, Is Required for Plasma Membrane Targeting of Gβγ. *Journal of Biological Chemistry* **278**, 17284-17290
55. Chicka, M. C., Hui, E., Liu, H., and Chapman, E. R. (2008) Synaptotagmin arrests the SNARE complex before triggering fast, efficient membrane fusion in response to  $\text{Ca}^{2+}$ . *Nat Struct Mol Biol* **15**, 827-835
56. Chapman, E. R., Desai, R. C., Davis, A. F., and Tornehl, C. K. (1998) Delineation of the Oligomerization, AP-2 Binding, and Synprint Binding Region of the C2B Domain of Synaptotagmin. *Journal of Biological Chemistry* **273**, 32966-32972
57. Mazzoni, M. R., Malinski, J. A., and Hamm, H. E. (1991) Structural analysis of rod GTP-binding protein, Gt. limited proteolytic digestion pattern of Gt with four proteases defines monoclonal antibody epitope. *J. Biol. Chem.* **266**, 14072-14081
58. Kozasa, T., and Gilman, A. G. (1995) Purification of recombinant G proteins from Sf9 cells by hexahistidine tagging of associated subunits. Characterization of  $\alpha_{12}$  and inhibition of adenylyl cyclase by  $\alpha_z$ . *Journal of Biological Chemistry* **270**, 1734-1741
59. Schindelin, J., Arganda-Carreras, I., Frise, E., Kaynig, V., Longair, M., Pietzsch, T., Preibisch, S., Rueden, C., Saalfeld, S., Schmid, B., Tinevez, J.-Y., White, D. J., Hartenstein, V., Eliceiri, K., Tomancak, P., and Cardona, A. (2012) Fiji: an open-source platform for biological-image analysis. *Nat Meth* **9**, 676-682
60. Schindelin, J., Rueden, C. T., Hiner, M. C., and Eliceiri, K. W. (2015) The ImageJ ecosystem: An open platform for biomedical image analysis. *Molecular Reproduction and Development* **82**, 518-529
61. Yim, Y. Y., Betke, K., and Hamm, H. (2015) Using Peptide Arrays Created by the SPOT Method for Defining Protein-Protein Interactions. in *Protein-Protein Interactions: Methods and Applications* (Meyerkord, C. L., and Fu, H. eds.), Springer New York, New York, NY. pp 307-320

## FIGURE LEGENDS

**Fig. 1. Supported lipid bilayer assay of Gβγ – t-SNARE interactions in membranes.** **A)** Fluorescently labeled Gβγ was assayed over a lipid bilayer using TIRF to isolate the fluorescence field to a band of approximately 100 nm above a cover slip. Anisotropy of the fluorescence emission was also assayed to confirm a Gbg interaction occurred. **B)** Gβ<sub>1</sub>γ<sub>1</sub> pressure ejected in a 1 s pulse (grey bar) over the bilayer containing t-SNAREs (produced from liposomes containing 130 t-SNAREs/vesicle) evoked a sustained increase in TIRF fluorescence. A similar pressure application over a bilayer lacking t-SNAREs showed a much smaller signal. Inset, increase in anisotropy after the pressure application ceased as flow in the chamber removed aqueous Gβγ but no increase in anisotropy after application over a bilayer lacking T-SNAREs (response 10.5±1.2%). The experiment was repeated 23 times. The mean change in anisotropy post-injection was  $r = 0.13 \pm 0.04$  for 8.8mM Gβ<sub>1</sub>γ<sub>1</sub> for membranes containing SNAREs. For membranes lacking SNARE, the magnitude of the change was  $Dr = 0.016 \pm 0.004$ , with a significance value of  $p = 0.02$  between the two conditions, Student's t-test. **(C)** The amplitude of fluorescence transients were measured first under epifluorescence to calibrate Gβγ concentrations applied from pressure ejection pipettes. **(Ci)** Output gave a signal proportional to the concentration of Gβγ applied and the signal ceased as the pressure application stopped. **(Cii)** in TIRF pressure application of Gβγ revealed a longer-lived response. This signal was normalized to the pressure applied concentration of Gβγ by dividing by the signal in Ci **(D)** Dose response curves were constructed from this normalized data (eg Cii) plotted against the dose calculated from (Ci). Gβ<sub>1</sub>γ<sub>1</sub> is depicted in blue ( $EC_{50} = 2.08 \pm 0.023 \mu M$ ,  $n = 4$  technical replicates) Gβ<sub>1</sub>γ<sub>2</sub> is depicted in green ( $EC_{50} = 147 \pm 71 nM$ ,  $n = 5$ ), and Gβ<sub>1</sub> K78A/W332Aγ<sub>2</sub> is depicted in red ( $EC_{50} = 86 \pm 50 nM$ ,  $n = 5$ ,  $p = 0.045$ , one-way ANOVA with Tukey's HSD test for each curve).

**Fig. 2. Ca<sup>2+</sup> enhances synaptotagmin 1 C2AB binding to t-SNARE-containing lipid bilayers, while Gβγ inhibits this interaction.** Recombinant synaptotagmin 1 C2AB domains were labeled on the single Cys residue in the primary sequence with Alexa Fluor 488-C<sub>5</sub>-maleimide. **A)** A lipid bilayer consisting of 55% PC, 15% PS, 29% PE, and 1% DiO containing t-SNARE complexes of syntaxin1A and SNAP-25 was maintained under solution containing Alexa Fluor 488-labeled syt1 (1μM) and imaged using polarized laser TIRF microscopy. Emission was detected with two PMTs orthogonally placed with respect to the polarization of the excitation beam. The traces show an example following the addition of 200μM Ca<sup>2+</sup> to the solution. Absolute fluorescence of the TIRF field increased as did anisotropy of the emission signal indicating binding of syt1 to the t-SNARE membrane. The subsequent addition of purified bovine Gβ<sub>1</sub>γ<sub>1</sub> (0.5μM) reduced both anisotropy and absolute fluorescence. **B)** Ca<sup>2+</sup> enhances the anisotropy signal of Alexa Fluor 488-labeled synaptotagmin 1 C2AB in a concentration-dependent manner ( $EC_{50} = 130 \pm 81 \mu M$ ). The experiment was performed three times for a total of three technical replicates.

**C)** Concentration-dependent inhibition of the anisotropy signal produced by Alexa Fluor 488-synaptotagmin 1 C2AB binding to t-SNARE complexes consisting of syntaxin1A and SNAP25 embedded in lipid membranes as in **Fig. 2A** at a Ca<sup>2+</sup> concentration of  $175 \pm 25 \mu M$ . The  $IC_{50}$  value for Gβ<sub>1</sub>γ<sub>1</sub> was  $0.7 \pm 0.3 \mu M$ . The experiment was performed three times for a total of three technical replicates. Error bars represent mean ± S. E. M.

**Fig. 3. Gβ<sub>1</sub> mutants that bind better to SNARE are less potent at inhibiting voltage-gated calcium channel currents.** HEK cells were transiently transfected with Ca<sub>v</sub>2.2 channels alone (control) or Ca<sub>v</sub>2.2 channels with wild type Gβ<sub>1</sub>, Gβ<sub>1</sub>K78A (K78A), Gβ<sub>1</sub>W332A (W332A), or Gβ<sub>1</sub>K78A/W332A (K78A/W332A) in addition to γ<sub>2</sub>. **A)** Representative whole cell currents ( $I_{Ca}$ ) recorded from a cell expressing Ca<sub>v</sub>2.2 channels and wild-type Gβ<sub>1</sub>γ<sub>2</sub>. The upper panel shows the voltage protocol consisting of two identical 20 ms steps to 0mV (P1 and P2) and the conditioning prepulse (50ms step to +120mV) prior to P2. The lower panel shows  $I_{Ca}$ . Note the current after the prepulse (P2) was much larger than



before the prepulse (P1) due to reversal of the tonic Gβγ-mediated inhibition. Also note the slow activation kinetics in P1, another characteristic of Gβγ-mediated inhibition that is reversed by the prepulse. The inset (bottom) shows superimposed P1 and P2 currents (normalized to the peak of P2) from a control cell and cells expressing the indicated Gβγ. **B)** Prepulse facilitation was determined at several test potentials (potential of P1 and P2 step) in control cells (no exogenous Gβγ) (n = 7) and cells transfected with Gβγ variants. Box and whisker plots denote the range of the individual data points (box denotes 25%, median, 75%; whiskers denote standard deviation of mean). At a test potential of -10 mV there was statistically significant prepulse facilitation produced by wild type Gβγ (n = 12, p < 0.001) and K78A (n = 5, p < 0.05) but not by W332A (n = 5) or K78A/W332A (n = 13) (one-way ANOVA with Dunnett's multiple pairwise comparison to control cells); at 0 mV test potential there was significant prepulse facilitation produced by wild type (n = 12, p < 0.001) and K78A (n = 5, p < 0.05) but not by W332A (n = 5) or K78A/W332A (n = 13) (one-way ANOVA with Dunnett's multiple pairwise comparison to control); at +10 mV test potential only wild type Gβγ produced significant prepulse facilitation (n = 12, p < 0.01) but not K78A (n = 5), W332A (n = 5), K78A/W332A (n = 13) (one-way ANOVA with Dunnett's multiple pairwise comparison to control); at +20 mV test potential only wild type Gβγ produced significant prepulse facilitation (n = 12, p < 0.01) but not K78A (n = 5), W332A (n = 5), K78A/W332A (n = 13) (one-way ANOVA with Dunnett's multiple pairwise comparison to control). ("ns" denotes not significantly different; \* p < 0.05; \*\* p < 0.01; \*\*\* p < 0.001; one-way ANOVA followed by Dunnett's multiple pairwise comparison to control).

**Fig. 4. Gβγ-derived peptides can perturb binding of full-length Gβ<sub>1</sub>γ<sub>2</sub> to SNAP25.** Alphascreen competition binding assays in which 20 nM biotinylated SNAP25 reacts with an EC<sub>80</sub> concentration of Gβ<sub>1</sub>γ<sub>2</sub> (180nM) to produce a luminescent signal(20) were conducted in the presence of peptides corresponding to primary sequences within Gβ<sub>1</sub> (A), Gγ<sub>1</sub>(B), and Gγ<sub>2</sub>(C) at varying concentrations (3.16 nM to 100μM) dissolved in DMSO. A value of 100% was assigned to the average of all conditions tested containing only DMSO as a positive control. The primary sequence of each peptide is depicted above the graph for each condition. Experiments were repeated three times. The following IC<sub>50</sub> values and 95% confidence intervals were observed: β<sub>1</sub> 328-337 IC<sub>50</sub> = 26μM (95% C.I: 17.0 to 37.8μM); Gγ<sub>2</sub> 2-24 : IC<sub>50</sub>= 3.81μM, (95% C.I: 24.4 to 5.95 μM); Gγ<sub>1</sub> 2-24 (IC<sub>50</sub>= 83.7μM, (95% C.I: 27.7μM to an upper limit greater than the highest concentration tested); Gγ<sub>1</sub> 8-25 IC<sub>50</sub>= 21.1μM (95% C.I: 12.2 to 36.2 μM ); Gγ<sub>2</sub> 9-28 IC<sub>50</sub>= 17.7μM, (95% C.I: 11.6 to 26.8 μM ).

**Fig. 5. Key regions for SNARE interaction upon Gβγ.** 3-dimensional X-ray crystallographic structure of either Gβ<sub>1</sub>γ<sub>1</sub>(45) (upper panels) or Gβ<sub>1</sub>γ<sub>2</sub> (46) (lower panel) containing key SNARE-binding regions obtained from Fig.3 and Fig. 4 highlighted in red. The key inhibitory residues K78 and W332 on Gβ<sub>1</sub> are highlighted in blue (upper left).

**Fig. 6. Gβ<sub>1</sub>γ<sub>1</sub> inhibits liposome fusion triggered by synaptotagmin 1 and Ca<sup>2+</sup> in a concentration-dependent manner.** **A)** Diagram showing assay principle. Synaptobrevin-bearing liposomes (containing approximately 50 copies/vesicle) containing the FRET pair NBD and rhodamine, covalently attached to PE, fuse with unlabeled liposomes containing t-SNARE complexes (containing approximately 130 copies/vesicle) consisting of syntaxin1A and SNAP-25. The increased surface area of the fused liposome reduces the quenching of NBD fluorescence by rhodamine and NBD fluorescence increases as a result. **B)** NBD fluorescence traces over time for synaptotagmin 1 (C2AB domain; 10 μM) and Ca<sup>2+</sup> (1 mM)-dependent liposome fusion in the presence of a series of concentrations of purified bovine Gβ<sub>1</sub>γ<sub>1</sub> (concentrations from 100 nM to 10 μM were tested). **C)** Maximum fluorescence values obtained for each concentration of Gβ<sub>1</sub>γ<sub>1</sub> and Gβ<sub>1</sub>γ<sub>2</sub>. An IC<sub>50</sub> value of 1.782 μM was obtained for Gβ<sub>1</sub>γ<sub>1</sub>-mediated inhibition of synaptotagmin-1 regulated fusion (95% C.I. 1.334 to 2.382μM), while the potency was

higher for  $G\beta_1\gamma_2$  with an  $IC_{50}$  value of 156.7nM (95% C.I 36.18 to 678.1nM). Conditions containing 0 nM  $G\beta_1\gamma_1$  were plotted at the 100 nM point. Experiments were performed three or four times for a total of three or four technical replicates for each condition tested. **D)** The condition containing no synaptotagmin 1 or  $G\beta_1\gamma_1$  was not different from the condition containing no synaptotagmin 1 and 10  $\mu$ M  $G\beta_1\gamma_1$  ( $p = 0.10$ , Student's t-test with Welch's correction). The condition lacking synaptotagmin 1 or  $G\beta_1\gamma_1$  was performed eleven times for eleven technical replicates, while the corresponding experiment with 10  $\mu$ M  $G\beta_1\gamma_1$  was performed four times for four technical replicates. **E)** Maximum fluorescence values obtained for each concentration of  $G\beta_1\gamma_1$  in the presence of either 10 $\mu$ M synaptotagmin 1 C2AB (blue line) or 3.16 $\mu$ M synaptotagmin 1 C2AB (orange line).  $G\beta_1\gamma_1$  was significantly more potent at 3.16 $\mu$ M synaptotagmin 1 C2AB, with an  $IC_{50}$  value of 987.5  $\mu$ M (95% C.I. 733nM to 1.330 $\mu$ M),

Figure 1

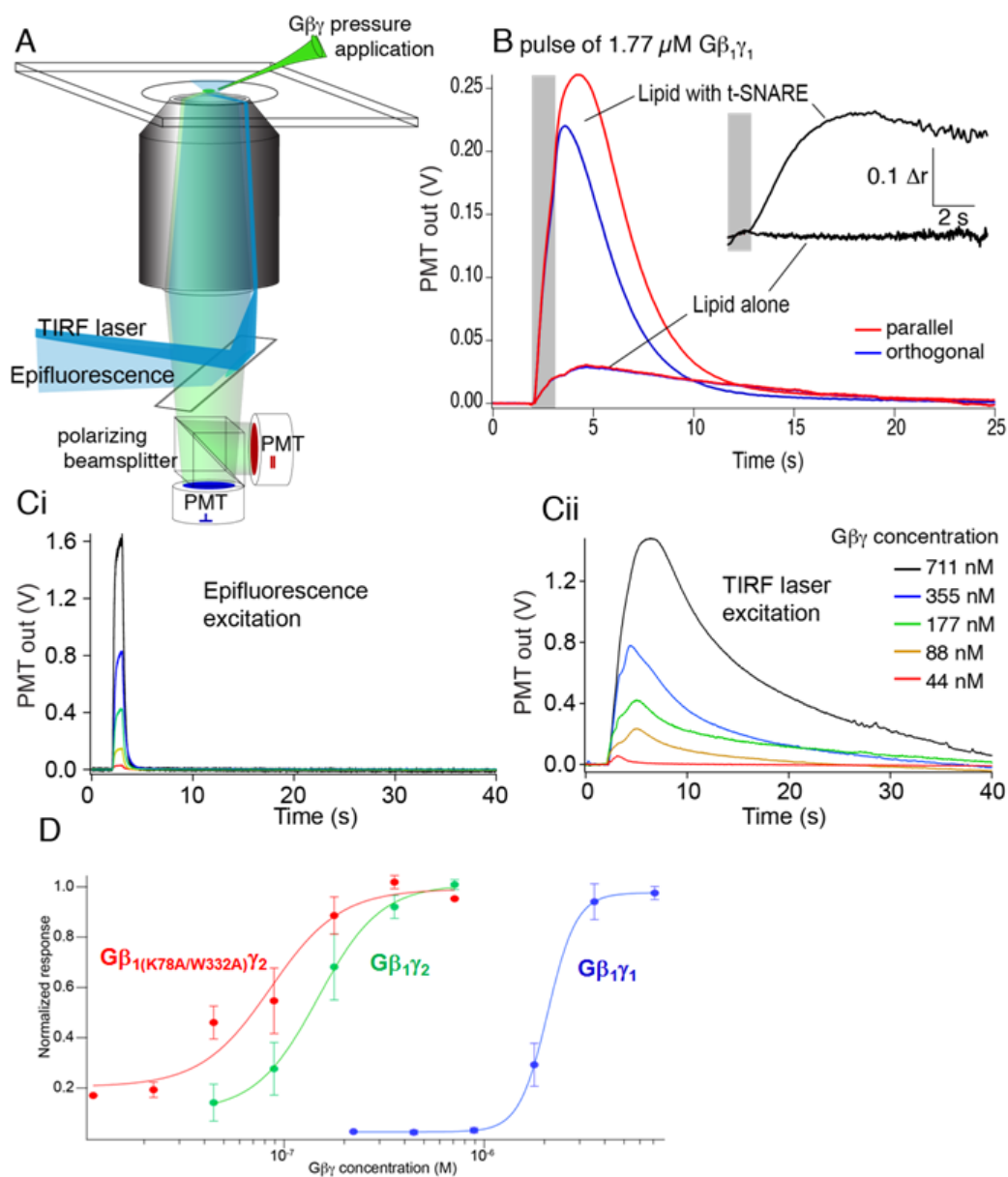


Figure 2

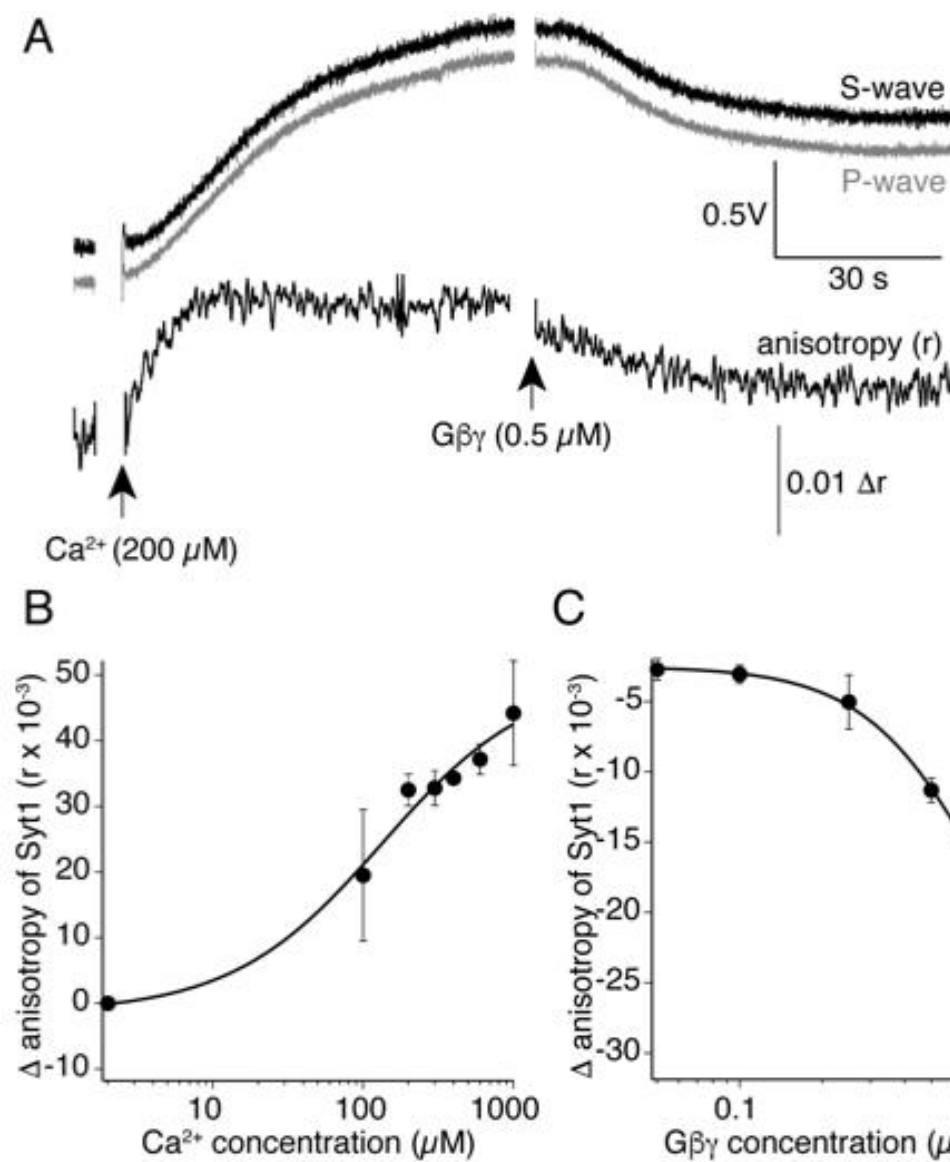




Figure 3

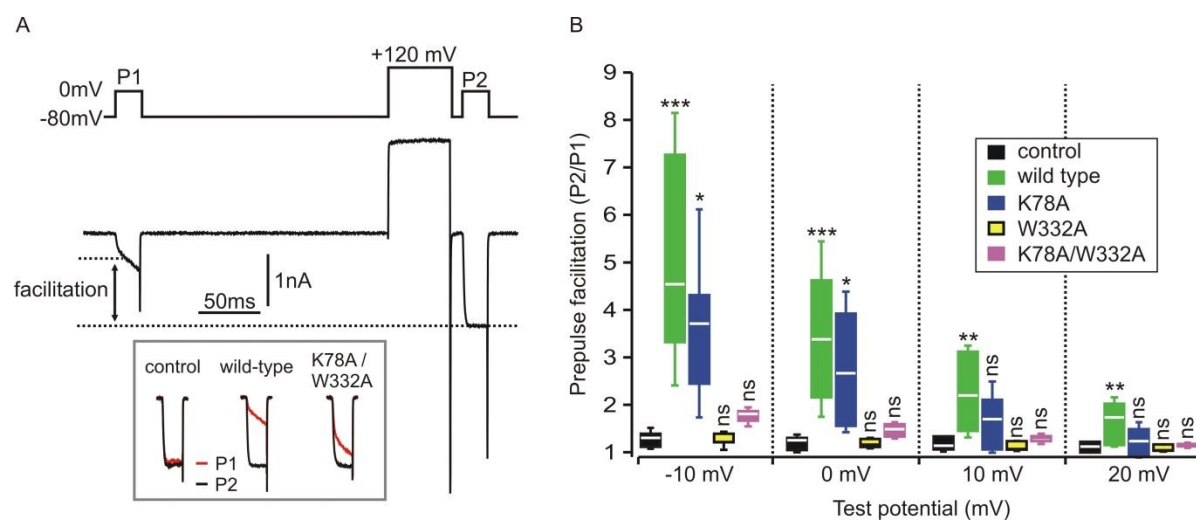


Figure 4

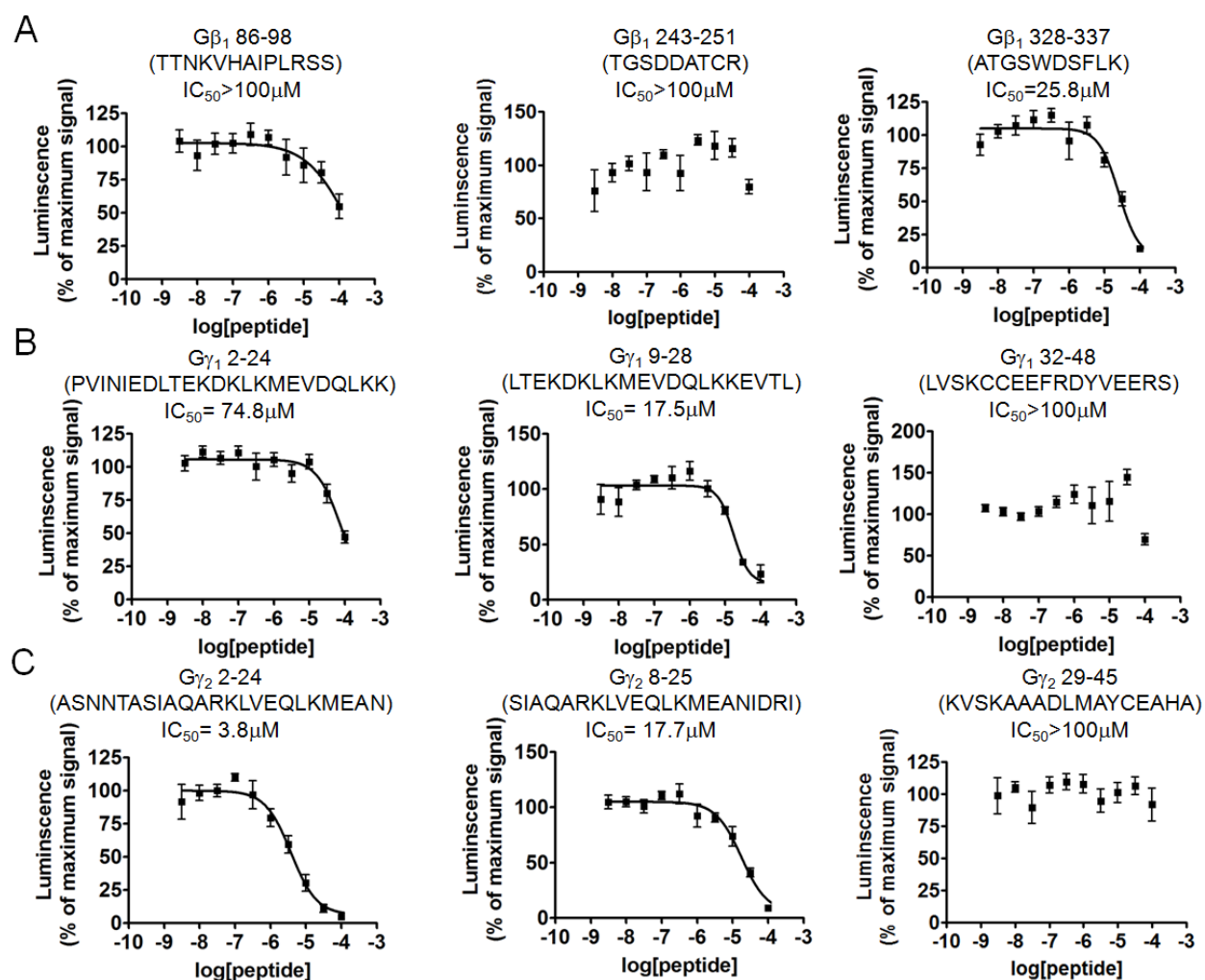


Figure 5

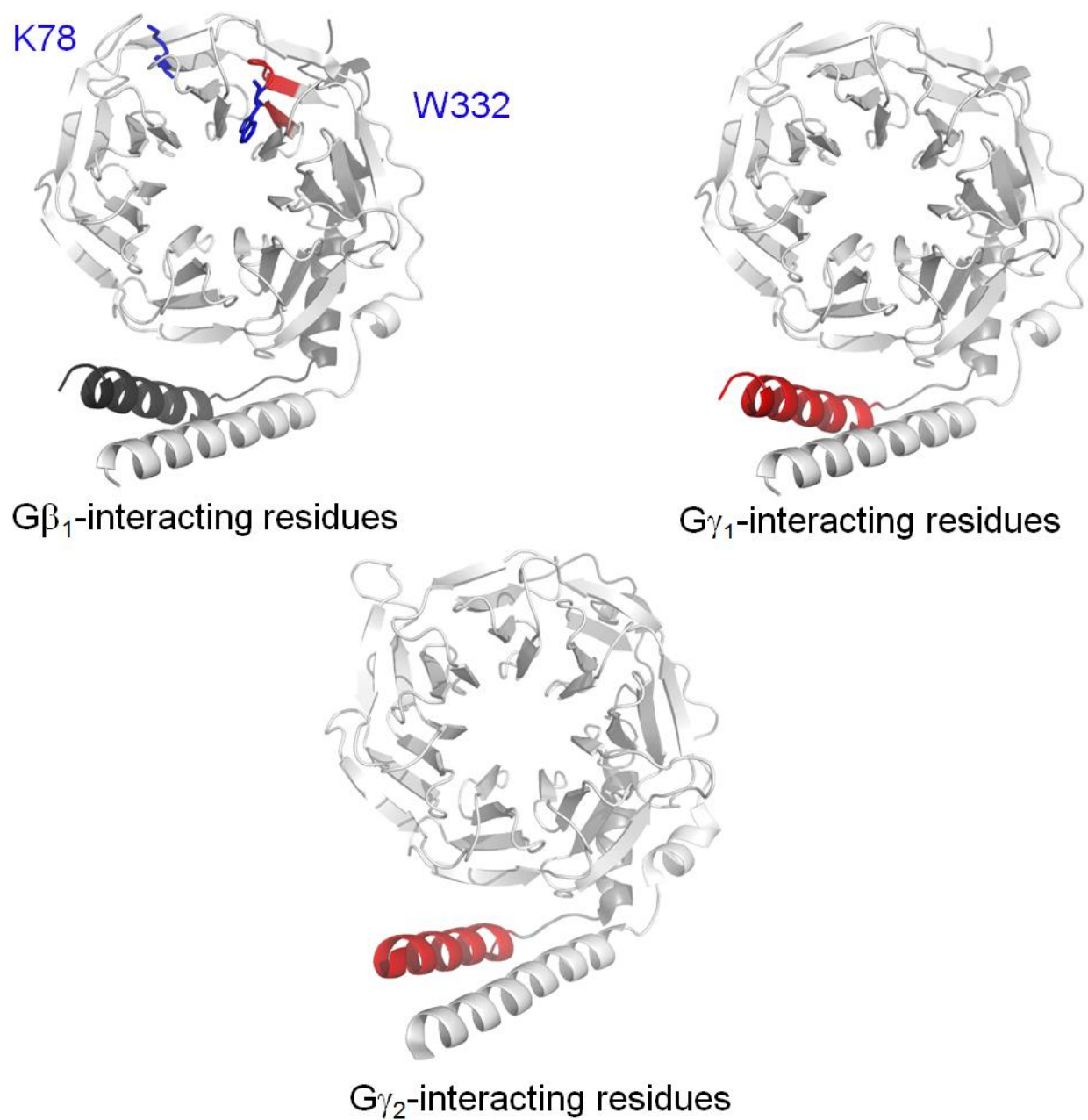
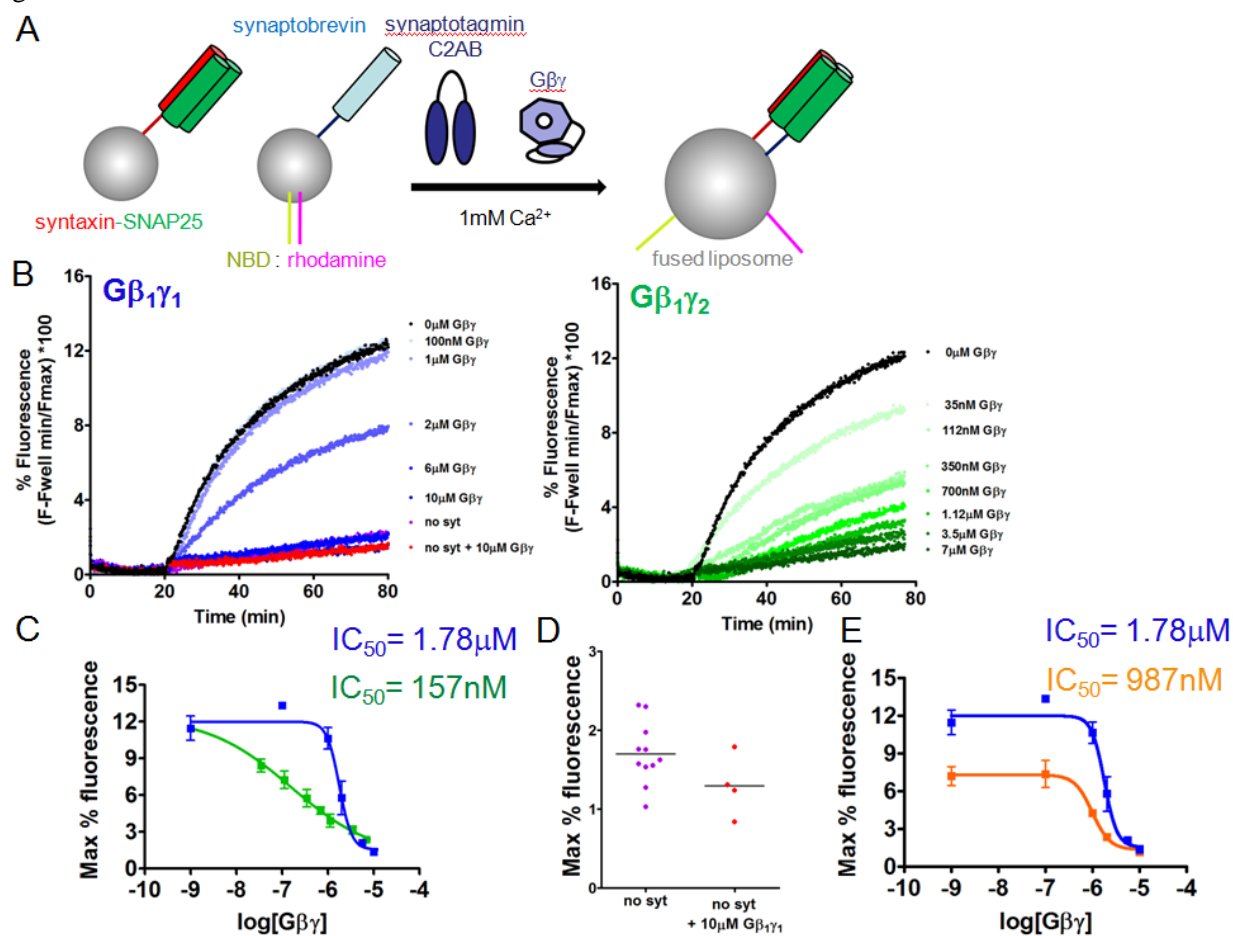


Figure 6





**Gβγ directly modulates vesicle fusion by competing with synaptotagmin for binding to neuronal SNARE proteins embedded in membranes.**

Zack Zurawski, Brian Page, Michael C. Chicka, Rebecca L Brindley, Christopher A Wells, Anita M Preininger, Karren Hyde, James A Gilbert, Osvaldo Cruz-Rodriguez, Kevin P. M. Currie, Edwin R Chapman, Simon Alford and Heidi E Hamm

*J. Biol. Chem.* published online May 17, 2017

---

Access the most updated version of this article at doi: [10.1074/jbc.M116.773523](https://doi.org/10.1074/jbc.M116.773523)

Alerts:

- [When this article is cited](#)
- [When a correction for this article is posted](#)

[Click here](#) to choose from all of JBC's e-mail alerts

This article cites 0 references, 0 of which can be accessed free at  
<http://www.jbc.org/content/early/2017/05/17/jbc.M116.773523.full.html#ref-list-1>